Prediction of energy absorption characteristics of aligned carbon nanotube/epoxy nanocomposites

2012 IOP Conf. Ser.: Mater. Sci. Eng. 40 012028

(http://iopscience.iop.org/1757-899X/40/1/012028)

IOP Conf. Series: Materials Science and Engineering **40** (2012) 012028 doi:10.1088/1757-899X/40/1/012028

Prediction of energy absorption characteristics of aligned carbon nanotube/epoxy nanocomposites

D Weidt[1,2,3], Ł Figiel[1,3] and M Buggy[2,3]

[1]Department of Mechanical, Aeronautical and Biomedical Engineering, University of Limerick, Ireland
[2]Department of Civil Engineering and Materials Science, University of Limerick, Ireland
[3]Materials & Surface Science Institute, University of Limerick, Ireland

E-mail: Lukasz.Figiel@ul.ie

Abstract. This research aims ultimately at improving the impact performance of laminates by applying a coating of epoxy containing carbon nanotubes (CNTs). Here, 2D and 3D computational modelling was carried out to predict energy absorption characteristics of aligned CNT/epoxy nanocomposites subjected to macroscopic compression under different strain rates (quasi-static and impact rates). The influence of the rate-dependent matrix behaviour, CNT aspect ratio and CNT volume fraction on the energy absorption characteristics of the nanocomposites was evaluated. A strong correlation between those parameters was found, which provides an insight into a rate-dependent behaviour of the nanocomposites, and can help to tune their energy absorption characteristics.

1. Introduction

Carbon fibre reinforced plastic (CFRP) laminates are commonly used in the aircraft industry because of their high specific stiffness, high specific strength, and good fatigue and corrosion resistance (when compared to metals). Unfortunately, they frequently behave as brittle materials when exposed to various types of impact loading as they cannot absorb/dissipate enough energy. As a result, matrix cracks can develop and in combination with a weak interlaminar strength, can lead to delaminations and catastrophic failure of CFRP-based structures.

Several attempts have been undertaken to enhance the damage and failure resistance of CFRP laminates by using carbon nanotubes (CNTs). This is due to CNT's excellent mechanical properties (e.g. stiffness, resilience) [1-2], their large specific surface area [3], and their ability to reinforce polymers at very low weight loadings. Hence, some researchers have used CNTs to enhance the matrix material's mechanical performance [4], others have used them to strengthen the interface between the CFRP pre-preg lamina [5], while others have grown them on the surfaces of fibres to produce a stitching effect [6].

We believe that the incorporation of a nanocomposite coating onto the laminate surface can help to enhance overall energy absorption characteristics of the laminates. This is to result from: (1) the large interfacial area of CNTs, which becomes potentially available for fracture propagation, CNT pull-out and crack bridging [7-9]; and (2) an enhanced nonlinear deformation of the nanocomposite matrix due to the presence of nanoparticles.

Therefore, the ultimate objective of this research project is to predict an impact response of CFRP laminates coated with CNT/epoxy nanocomposites using multiscale modelling validated by experiments [10]. This study is a part of our project, and it is focused on the prediction of mechanical behaviour of aligned CNT/epoxy nanocomposites across different strain rates. In particular, the emphasis is on the influence of aligned CNTs on the compressive macroscopic stress-strain response of the CNT/epoxy nanocomposite at strain rates ranging from quasi-static to impact rates. They are then used to evaluate energy absorption characteristics of the nanocomposites. For this, a nonlinear and rate-dependent constitutive model for epoxy is implemented into the finite element (FE) framework (ABAQUS), and combined with the representative volume element (RVE) and numerical homogenisation. FE predictions of the nanocomposite response at different strain rates are compared with unfilled epoxy, to demonstrate the effect of CNTs (aspect ratio, volume fraction) on energy absorption characteristics of CNT/epoxy nanocomposites.

2. Modelling methodology

It was assumed that the macroscopic response of the nanocomposite can be predicted using the RVE concept and numerical homogenization. For that purpose it was assumed that the continuum theory holds down to the scale at which the nanocomposite morphology can be captured with an RVE. This offers a compromise between accuracy and computational time.

It was further assumed that the CNT morphology is globally periodic and that the macroscopic deformation is uniform. This enabled the application of RVEs with imposed periodic boundary conditions. Two types of RVEs were considered here (see Figure 1): (1) simple axisymmetric RVE (A) and (2) three-dimensional cuboidal (3D) RVE (B). The axisymmetric RVE was used because of its simplicity, and ability to capture regular, well dispersed morphologies of CNTs. On the other hand, the 3D RVE was chosen to account for an irregular morphology of randomly distributed and aligned CNTs. A cuboidal RVE was chosen over a cubic RVE in this work because of the assumed length of CNTs, CNT volume fraction and a small number of CNTs (10). 3D RVEs were generated using an in-house developed Python script.

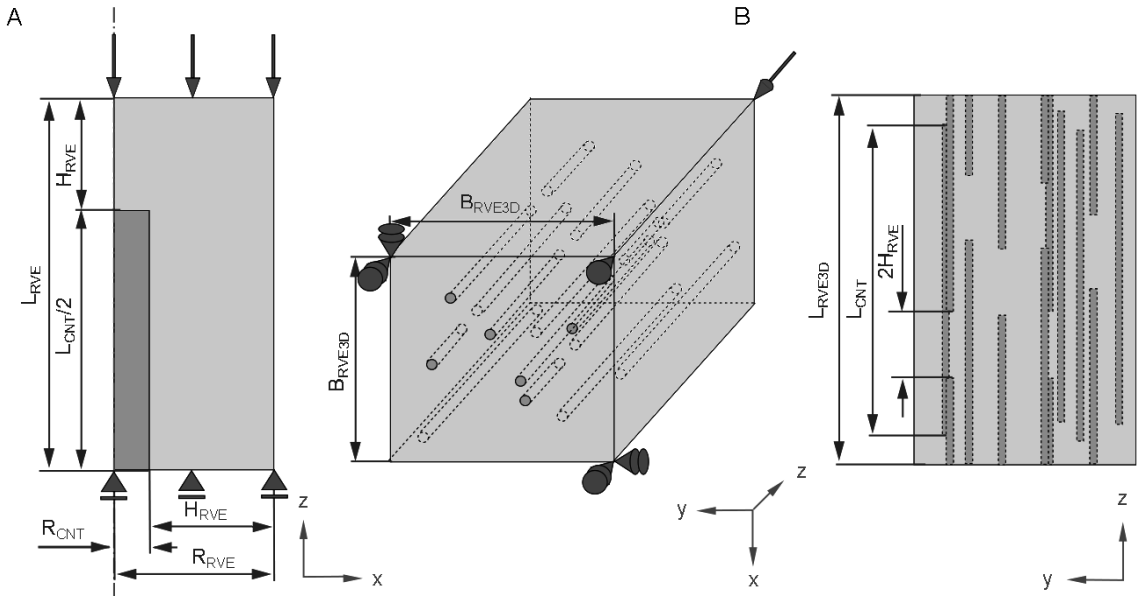

Figure 1. Axisymmetric (A) and three-dimensional RVE (B) of CNT/epoxy nanocomposites; Epoxy matrix (light grey), homogenised CNT (medium grey), boundary conditions (dark grey).

Homogenised CNTs with effective elastic properties were used in this work as computationally more efficient than their dicrete tubular continuum counterparts. In order to calculate the effective elastic properties of CNTs, the following formula was used:

$$E_{CNT}^{eff} = E_{CNT} \frac{2R_{CNT}T_{CNT} - T_{CNT}^2}{R_{CNT}^2} \quad (1)$$

where E_{CNT}, R_{CNT} and T_{CNT} are the Young modulus, outer radius and thickness of a discrete CNT, respectively. In this work, E_{CNT}=3.36TPa was used as obtained from the elastic shell theory for the given wall thickness T_{CNT}=0.1nm and Poisson's ratio of ν=0.2 [12]; the outer radius of the CNTs was assumed to be equal to R_{CNT} =5nm. The effective Young modulus of homogenised CNTs was calculated from Eq. (1) to be 133.056GPa in both axial and transverse directions. However, it must be mentioned that Eq. (1) was derived based on the axial CNT direction. Hence, this is only an approximation to the transverse response of CNTs. In our former study [11], we found negligible differences between the stress-strain response of RVEs with homogenised CNTs and their discrete counterparts. However, this result was obtained from simulations on RVEs with perfectly aligned CNTs under compressive loading in CNT axis direction [11], and it will be verified in the future for randomly oriented CNTs.

Perfect bonding between CNTs and the matrix was assumed in this work. Hence, a possible debonding and pull-out of CNTs from the matrix was excluded as possible energy dissipation/absorption mechanisms. As a result, plastic deformation of the epoxy matrix was expected to be the major cause of energy absorption.

The non-linear and rate-dependent matrix behaviour was represented using a physically-based constitutive model proposed by Buckley et al. [13] for thermosetting resins. The model accounts for the strain softening and adiabatic heating effect (active upon applied impact loads), and enabled capturing basic phenomena of epoxy matrices subjected to varying strain rates. The mechanical constitutive behaviour was implemented as a user subroutine UMAT (ABAQUS/Standard), with the model parameters obtained by Buckley et al [13,14] for the standard bisphenol A resin.

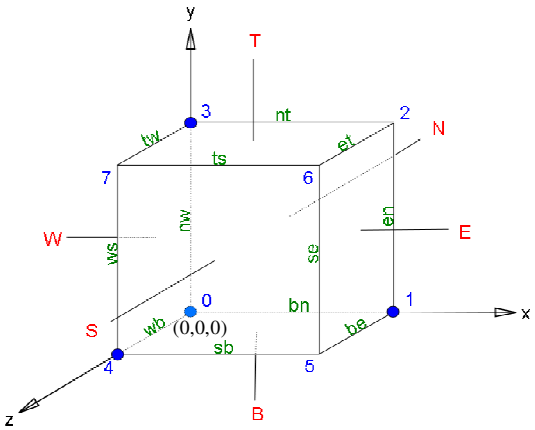

Figure 2. Schematic of a 3D RVE with notations of faces (N, W, S…), edges (nt, tw, ts…) and corner nodes (0,1,2…); periodic boundary conditions were applied according to equation (2); in addition, displacements were applied/constrained at corner nodes 0, 1, 3 and 4 (as shown in Figure 1), e.g. corner node 0 at (x,y,z)=(0,0,0) is constrained in all directions to exclude rigid body motion.

Uniform displacement boundary conditions were applied to the axisymmetric RVE in the y-direction – uniform deformation of the right edge in the x-direction (see Figure 1A) was enforced by setting the corresponding nodal displacements (right edge) as equal to the top right corner node of the RVE (using the ABAQUS '*Equation' command).

The complete set of periodic boundary conditions (PBCs) was used for 3D RVEs as follows:

$$\boldsymbol{u}_F^+ - \boldsymbol{u}_F^- = \boldsymbol{u}_{(I)}^+ - \boldsymbol{u}_{(I)}^-, \text{ and } \boldsymbol{u}_E^+ - \boldsymbol{u}_E^- = \boldsymbol{u}_{(I)}^+ - \boldsymbol{u}_{(I)}^- \text{ and } \boldsymbol{u}_{(I)}^+ - \boldsymbol{u}_{(I)}^- = \boldsymbol{u}_{(J)}^+ - \boldsymbol{u}_{(J)}^- \quad (2)$$

where $\boldsymbol{u}_F$ and $\boldsymbol{u}_E$ are the displacement vectors of face and edge nodes, while $\boldsymbol{u}$ with the subscript I or J refers to a corner node; symbols '+' and '-' represent two opposite faces, edges or nodes of the RVE. In addition, external nodal displacements representing macroscopic deformations (macroscopic compressive strains) were applied to relevant corner nodes (1, 3 and 4 – see Figure 2). Those boundary conditions result in tractions $\boldsymbol{t}$ (due to PBCs) and nodal forces $\boldsymbol{f}$ (due to external displacements) acting on the RVE. The macroscopic Cauchy stresses $\boldsymbol{\sigma}_M$ can then be calculated as follows [15]:

$$\boldsymbol{\sigma}_M = \frac{1}{V_{RVE}} \int_{V_{RVE}} \boldsymbol{\sigma}_{RVE}(\boldsymbol{x})\, dV = \frac{1}{V_{RVE}} \sum_I \boldsymbol{f}_{(I)} \otimes \boldsymbol{x}_{(I)}\,, \tag{3}$$

where V_{RVE} is the current volume of an RVE, and $\boldsymbol{f}_{(I)}$ and $\boldsymbol{x}_{(I)}$ are current nodal forces and nodal positions of a corner node *I*. For the macroscopic compressive strains applied uniaxially in the z-direction (see Figure 2), the resulting stresses in z-direction, σ_{zz}, can be calculated from Eq. (3) as $\sigma_{zz} = V_{RVE}^{-1} f_{z(4)} x_{z(4)}$, where $f_{z(4)}$ and $x_{z(4)}$ denote force and position of the node 4 (see Figure 2).

The axisymmetric RVEs (matrix and CNTs) were discretized using 8-node quadratic axisymmetric quadrilateral elements CAX8. 3D RVEs were discretized using 10-node quadratic tetrahedron elements C3D10 (matrix region) and 20-node quadratic brick elements C3D20 (CNT region). CNT and matrix regions were tied together via surface-based tie constraints.

3. Results and discussion

Predicted compressive stress-strain curves and energy absorption characteristics of CNT/epoxy nanocomposites subjected to different strain rates are shown and discussed in this section.

Effects of CNT volume fraction (VF) and varying strain rates on the stress-strain response are shown in Figure 3. As expected, the incorporation of CNTs into epoxy produced a considerable stiffening effect in the linear portion of the curve – the Young modulus of the nanocomposite increased by around 15%, 30%, 46% and 77% (CNT VF of 0.5%, 1%, 1.5% and 2.5%, respectively) compared to pure epoxy. Hence, CNT loading exhibits almost a linear effect on the Young modulus of the nanocomposite. As expected, no change in the nanocomposite Young's modulus was predicted with increasing strain rate. This is because the constitutive model for epoxy used in this work does not account for the rate-dependent stiffness. However, experimental data across a wide range of compressive strain rates for an RTM-6 epoxy system reported in Gerlach et al. (2008) [16] shows that there is no significant change in Young's modulus up to true strain rates ~ 10^3 s^{-1}. The latter is greater than the maximum magnitude of nominal strain rates considered in this work, as the true strain rate $\dot{\varepsilon}_M$ is related to the applied (nominal) strain $\dot{\varepsilon}_{M(app)}$ through $\dot{\varepsilon}_M = \dot{\varepsilon}_{M(app)} / \left(1 + \varepsilon_{M(app)}\right)$.

The stiffening effect caused by CNT loading on the stress response continues beyond the elastic limit - for the given magnitude of applied strain, a gradual increase in the macroscopic true stress with CNT loading was predicted. Moreover, the start of nonlinear deformation is shifted to a slightly lower value of applied strain with increasing CNT volume fraction – in all cases a higher yield stress is predicted when compared with the pure epoxy.

The post-yield strain softening, which was predicted (and validated experimentally [13]) for the pure epoxy, is no longer present for VF equal to or greater than 1%. Furthermore, an increase in the CNT VF resulted in an increased post-yield strain-hardening effect. Hence, assuming that the energy absorbed by the material system can be represented by the area under the stress-strain curve, it is postulated that the improved post-yield behaviour of the nanocomposite can largely contribute to the improved energy absorption of the CNT/epoxy nanocomposite in compression. This increase in energy absorption characteristics results from an enhanced nonlinear deformation (pronounced by strain stiffening) of the matrix, caused by the presence of CNTs.

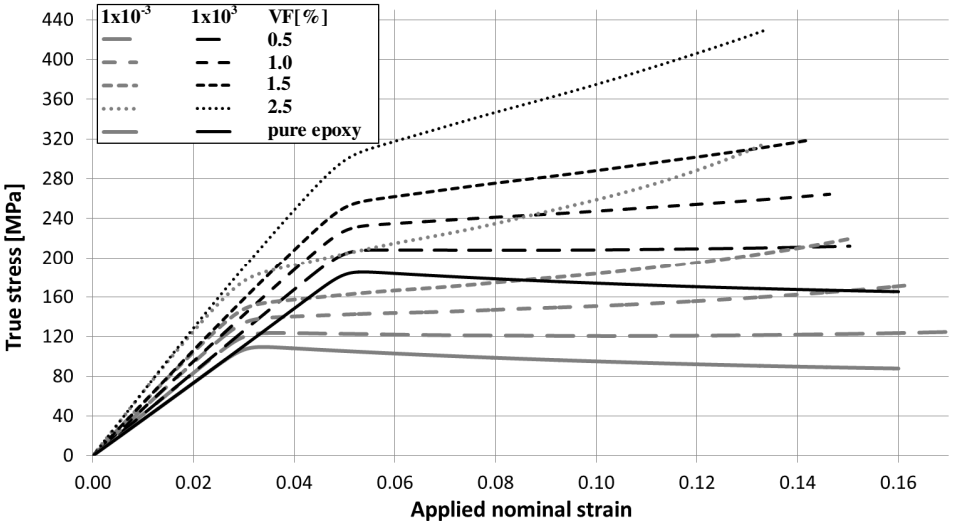

Figure 3. Predicted stress-strain curves for pure epoxy and nanocomposites for different CNT volume fractions (VF) and applied strain-rates; results obtained from axisymmetric RVEs; CNT aspect ratio AR=50.

Effects of CNT aspect ratio (AR) and varying strain rates on the stress-strain were also investigated. In general, qualitatively similar trends were found as for the case of increasing CNT loading. However, quantitatively, only a slight increase of the nanocomposite modulus was predicted with increasing CNT AR within the investigated range from 50 to 250. As indicated by different curves, the effect of CNT AR on the stress-strain response tends to saturate with increasing aspect ratio - less significant improvement of the overall stress-strain response was obtained for aspect ratios greater than 100. However, in general there is an enhanced post-yield behaviour (increasing strain stiffening) with increasing CNT AR, which suggests that energy absorption characteristic are enhanced only at large deformations. Again, the major contribution to that comes from the enhanced nonlinear deformation (strain stiffening) of the matrix caused by the CNT presence.

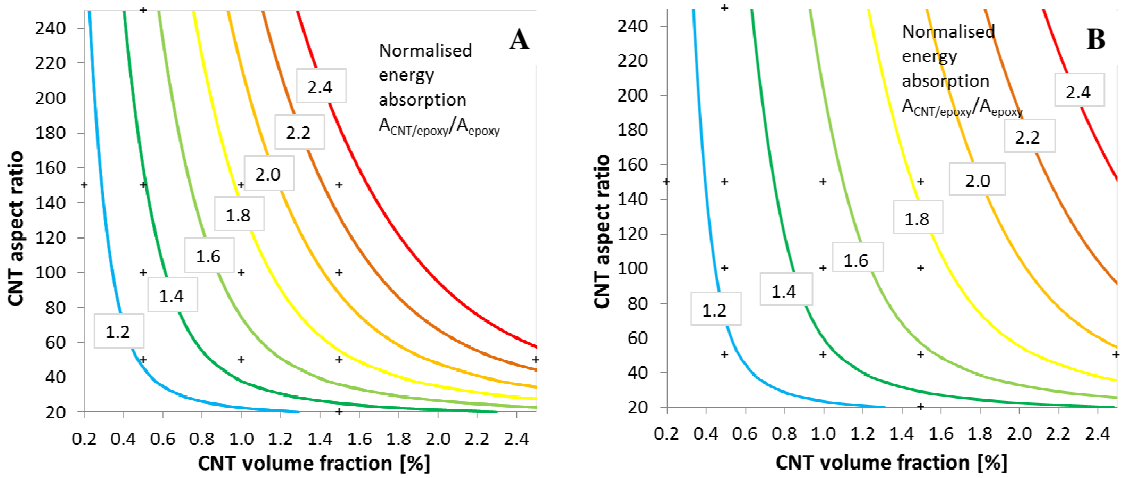

Figure 4. Predicted normalised energy absorption characteristics as a function of CNT aspect ratio (AR) and CNT volume fraction (VF) for quasi-static $1x10^{-3}$ s^{-1} (A) and high strain rates $1x10^{3}$ s^{-1} (B). The normalised energy absorption characteristics at the data points (crosses) were used to determine the coefficients of the nonlinear regression functions via the least squares method.

Normalised energy absorption characteristics were then evaluated based on the compressive stress-strain curves. Areas under those curves were evaluated up to strains ~13%, both for the nanocomposites and matrix, at two strain rates ($1x10^{-3}s^{-1}$ and $1x10^{3}s^{-1}$), and with different volume fractions and aspect ratios. Our predictions are shown in Figure 4, where, in general, the normalised energy absorption is enhanced due to the presence of CNTs at both strain rates. A significant correlation between CNT aspect ratio and CNT volume fraction is predicted - an increase in CNT volume fraction contributes to a considerable increase in normalised energy absorption under quasi-static loading ($1x10^{-3}s^{-1}$) for CNT aspect ratios AR=150. In comparison, predictions for aspect ratios AR=50 do not show such a significant increase in the normalised energy absorption with increasing volume fraction. Hence, our results suggest what CNT loading must be used for a given average CNT aspect ratio to improve the energy absorption of CNT/epoxy nanocomposites. This is under the assumption that the nonlinear matrix deformation is the primary energy absorption mechanism. Future studies will include other mechanisms such as debonding [10] and pull-out of CNTs from the matrix.

4. Conclusions

Computational modelling carried out here for aligned CNT/epoxy nanocomposites subjected to different compressive strain rates demonstrated: (1) increase of the nanocomposite stiffness; (2) strain stiffening in the post-yield regime; and (3) the improvement of energy absorption characteristics, with increasing CNT volume fraction and CNT aspect ratio.

Acknowledgements

The project is supported by the Irish Research Council for Science, Engineering and Technology. Computational facilities are provided by the Irish Centre for High-End Computing.

References

[1] Treacy M M J, Ebbesen T W and Gibson J M 1996 *Nature* **381** 678-680
[2] Cooper C A, Young R J and Halsall M 2001 *Compos. Part A-Appl. S.* **32** 401-411
[3] Peigney A, Laurent Ch, Flahaut E, Bacsa R R and Rousset A 2001 *Carbon* **39** 507-514
[4] Yokozeki T, Iwahori Y, Ishiwata S and Enomoto K 2007 *Compos. Part A-Appl. S.* **38** 2121-2130
[5] Hu N, Li Y, Nakamura T, Katsumata T, Koshikawa T and Arai M 2012 *Compos. Part B-Eng.* **43** 3-9
[6] Wicks S S, de Villoria R G and Wardle B L 2010 *Compos. Sci. Technol.* **70** 20-28
[7] Gojny F H, Wichmann M H G, Fiedler B and Schulte K 2005 *Compos Sci Technol* **65** 2300-2313
[8] Zhang W, Picu R C and Koratkar N 2007 *Appl. Phys. Lett.* **91** 193109
[9] Wernik J M and Meguid S A 2010 Appl. Mech. Rev. **63** 050801 **70** 20-28
[10] Weidt D, Figiel Ł and Buggy M 2012 *Mater. Sci. Forum* **714** 3-11
[11] Weidt D, Figiel Ł and Buggy M 2012 *Proc. 15th Int. Conf. of Deformation, Yield and Fracture of Polymers (Kerkrade, the Netherlands, 1-5 April 2012)* pp 278-281
[12] Wang C Y and Zhang L C 2008 *Nanotechnology* **19** 195704
[13] Buckley C P, Dooling P J, Harding J and Ruiz C 2004 *J. Mech. Phys. Solids* **52** 2355-2377
[14] Buckley C P, Harding J, Hou J P, Ruiz C and Trojanowski A 2001 *J. Mech. Phys. Solids* **49** 1517-1538
[15] Figiel Ł, Dunne F P E, Buckley C P 2010 *Modelling Simul. Mater. Sci. Eng.* **18** 015001
[16] Gerlach R, Siviour C R, Petrinic N, Wiegand J 2008 *Polymer* **49** 2728-2737